

Preparation of Bi Substituted Yttrium Orthoferrite Nanopowders by Sol- Gel Method and Investigation of Their Magnetic Properties

A. Beiranvand¹, M. Mehdipour¹, J. Amighian², A. Yousif³ and M. Mozaffari²

¹. Department of Physics, Faculty of Science, Korram Abad branch, Islamic Azad University, Korram Abad, Lorestan, Iran.

². Department of Physics, Faculty of Science, University of Isfahan, Isfahan, Iran.

³. Department of Physics, College of Science, Sultan Qaboos University, P.O. Bax 36, PC123, Muscat, Sultanate of Oman. a.beyranvand@gmail.com

Abstract: Nanopowders of $Y_{1-x}Bi_xFeO_3$ ($x=0.0, 0.1, 0.15$ and 0.2) have been synthesized by the sol gel method. X-ray diffraction identifications show that all the samples have orthorhombic structure and mean crystallite sizes of the nanopowders are in the range of 40 nm, using Scherrer's formula. Mean particle sizes of the samples were obtained by TEM, which is in the range of 75 nm. The ^{57}Fe Mössbauer spectra of $Y_{1-x}Bi_xFeO_3$ nanopowders at 78 and 295 K have been recorded and the results show that all the Fe^{3+} ions are almost at the symmetrical positions. Room temperature magnetization measurements show that with increasing Bi content up to 0.15, the magnetization increases, whereas it decreases for the sample with $x=0.2$. M-T curves of the samples were recorded at applied fields of 40 and 13500 Oe. Although all samples show a metamagnetic behavior around $T_k=225$ °C and at higher applied field, but for the sample with $x=0.2$, the behavior is more clear. [A. Beiranvand, M. Mehdipour, J. Amighian, A. Yousif and M. Mozaffari. **Preparation of Bi Substituted Yttrium Orthoferrite Nanopowders by Sol- Gel Method and Investigation of Their Magnetic Properties.** *Life Sci J* 2013;10(5s):155-161] (ISSN:1097-8135). <http://www.lifesciencesite.com>. 28

Keywords: nanopowder; sol-gel method; metamagnetism; Mössbauer spectra.

Introduction:

Orthoferrites have the formula $RFeO_3$, which R is either a rare earth atom or yttrium. Their space group is Pb_{nm} , which is a distorted perovskite. The crystallographic unit cell, shown in Fig.1, contains four equivalent iron ions. The distortion of the perovskite structure is such that the iron environment remains essentially octahedral; however, the axes of the four octahedral sites are in different directions. The environment of the ions is, however, far from cubic [1].

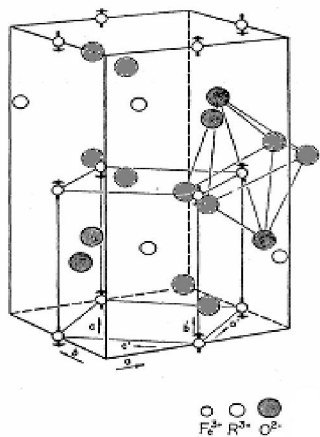


Fig. 1. the unit cell of the orthoferrites $RFeO_3$

The structure can be visualized as a three-dimensional network of strings of FeO_6 octahedra.

One of the anions (O^{2-}) forms the common apex of the two adjacent octahedra and provides the superexchange force to six nearest neighbors [2]. Below T_N , the system is antiferromagnetically ordered, with a slight canting of Fe spins giving rise to a weak-ferromagnetic moment that dominates the magnetic behavior of the system. The origin of the canting is the antisymmetric exchange Dzyaloshinsky-Moriya (DM) interaction $-\mathbf{D} \cdot (\mathbf{M}_1 \times \mathbf{M}_2)$, where \mathbf{D} is the DM vector and \mathbf{M}_1 and \mathbf{M}_2 are the sublattice magnetizations [3]. In orthoferrites with diamagnetic R ions, La^{3+} , Y^{3+} , Lu^{3+} , the measured ferromagnetic moment M is totally due to canting. The canting angle α at zero external field is given by:

$$\alpha = \frac{M}{2M_0} \quad (1)$$

where M_0 is the iron sublattice moment, assuming that $M_0=5 \mu_B$ [4].

The rare-earth orthoferrites crystallize in the perovskite structure and find applications in various areas such as solid oxide fuel cell, sensors and catalysis [5-7]. Single phase orthoferrites are difficult to prepare with the conventional ceramic method. Fine powders of orthoferrites are desirable for these applications which can be prepared by coprecipitation [8], hydrothermal [9] and sol-gel methods [2]. Wet-chemical methods are promising to produce nanoparticles with narrow size distribution.

The aim of this work was to synthesize single phase $Y_{1-x}Bi_xFeO_3$, using sol-gel method and to investigate the magnetic properties in the prepared orthoferrite nanopowders.

Experimental Design:

Nanopowders of the $Y_{1-x}Bi_xFeO_3$ ($x=0, 0.1, 0.15$ and 0.2) orthoferrites have been synthesized by sol-gel method from high-purity citric acid, $Fe(NO_3)_3 \cdot 9H_2O$, $Y(NO_3)_3 \cdot 5H_2O$ and $Bi(NO_3)_3 \cdot 5H_2O$ raw materials, all from Merck Co. Germany. To prepare the samples aqueous solutions of 2M citric acid and proper moles of the salts were mixed and stirred on a hot plate magnet to about $55^\circ C$ to avoid precipitation and obtain homogeneous mixtures. At this stage ethylene glycol was added into each solution with a proportion of citric acid/ethylene glycol ratio of 70:30 and heated to $80^\circ C$, until different gels were formed. The gels were dried at $110^\circ C$ for about 48 h to obtain xerogel powders. The powders were calcined in air for 4 h at temperatures of $850^\circ C$ for $x=0, 0.1$ and 0.15 and $750^\circ C$ for $x=0.2$.

Crystal structures and morphologies of the nanopowders were investigated by an x-ray diffractometer (Bruker D8 ADVANCED) and a transition electron microscope (TEM) was performed using a JEOL (1200EX) system equipped with an

AMT digital camera operating at an accelerating high voltage of 120kV respectively. The crystallite sizes were determined from peaks broadening of the XRD patterns, using Scherrer's formula. Magnetic measurements were carried out using a DMS 1660 vibrating-sample magnetometer (VSM) in magnetic fields up to 13.5 kOe and temperature range of 298-773K. Mossbauer spectra of the samples were obtained at 78 and 295 K, using a constant acceleration Mossbauer spectrometer with 50 mCi ^{57}Co Rh source. The low temperature measurement was performed using a liquid nitrogen flow cryostat. The spectrometer was calibrated with α -Fe foil spectra at room temperature. The measured data were analyzed using a non-linear least-squares fitting program assuming Lorentzian lines.

Results and discussion:

XRD patterns of the $Y_{1-x}Bi_xFeO_3$ ($x=0, 0.1, 0.15$ and 0.2) nanopowders indicate that all the samples have a single phase orthorhombic structure, Fig. 2. The lattice parameters of the samples are given in Table 1, which shows that by increasing Bi content the lattice parameters are increased. This is due to the fact that ionic radius of Bi^{3+} (1.03 \AA) is larger than that of Y^{3+} (0.90 \AA) [10]. A mean crystallite size of about 40 nm was obtained for all the samples.

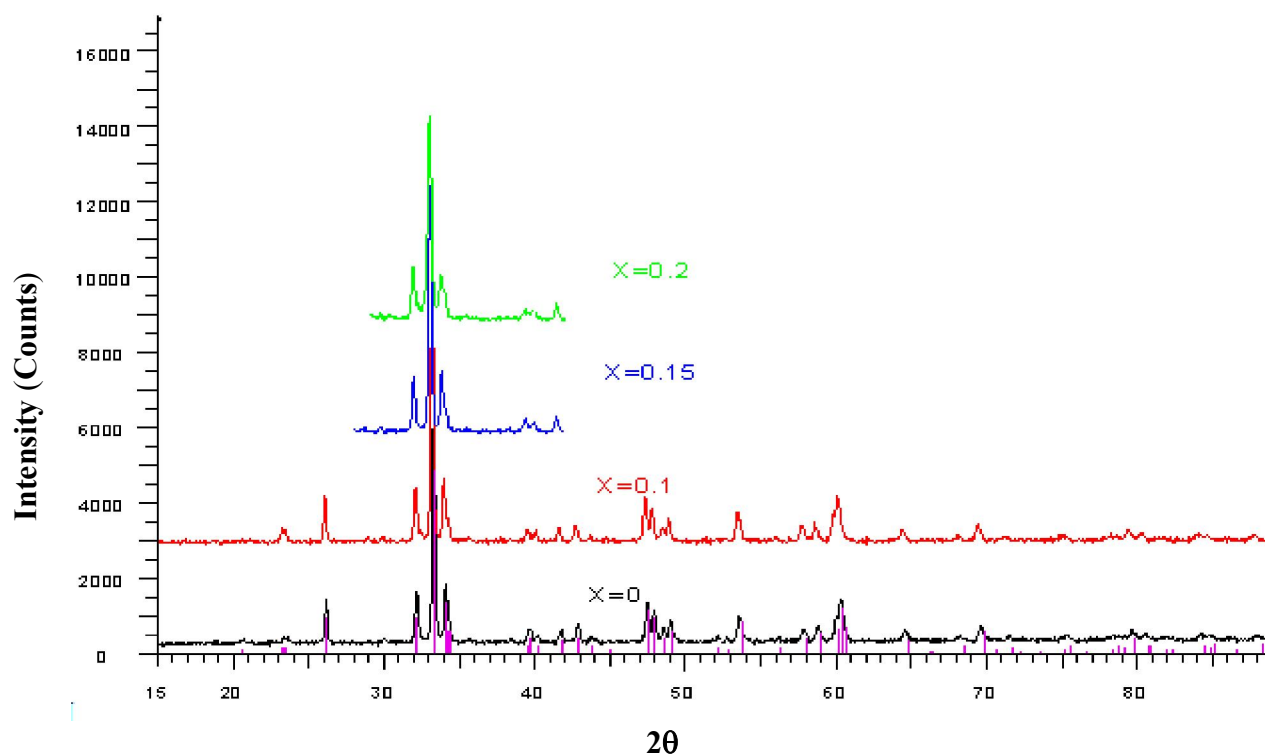


Fig. 2. XRD patterns of the samples.

Table.1 Lattice parameters of $Y_{1-x}Bi_xFeO_3$ nanopowders.

c (Å)	b (Å)	a (Å)	x
5.257	7.577	5.562	0.0
5.275	7.59.5	5.579	0.10
5.292	7.63	5.597	0.15
5.308	7.659	5.60	0.20

Fig. 3 shows the Mössbauer spectra of all the samples at 78 and 295 K. All spectra show sextets characteristic, indicating that all samples have magnetic order. The Mössbauer parameters extracted from the spectra are given in Table 2, which for $x=0.0$ is in consistent with the previously reported values on $YFeO_3$ [2].

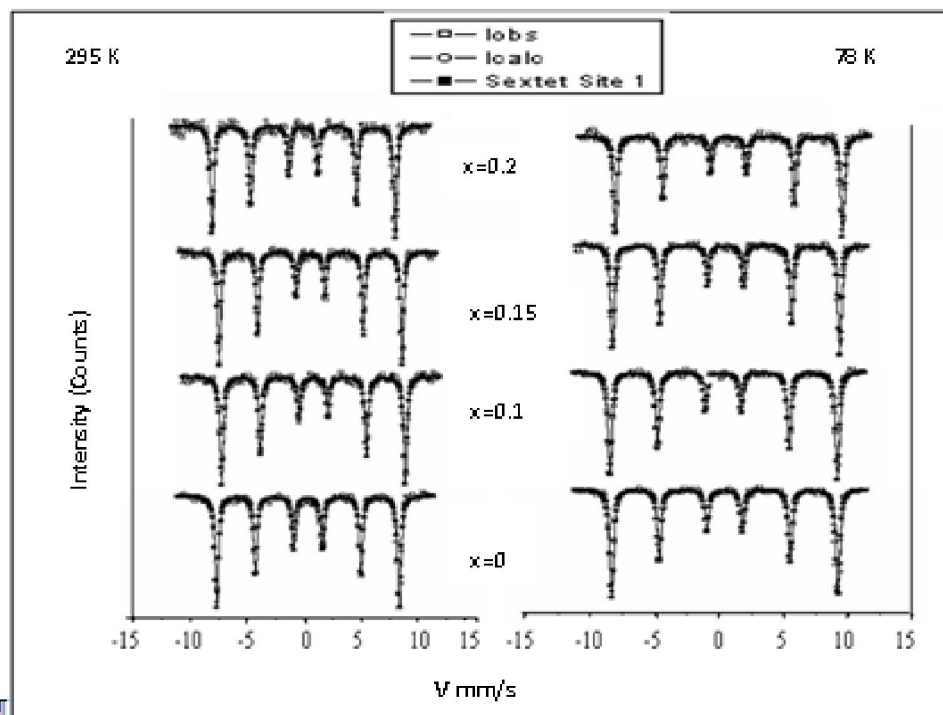


Fig. 3. Mössbauer spectra of the samples with different x values at 295 and 78 K.

Table 2. The Mössbauer parameters of $Y_{1-x}Bi_xFeO_3$ at 78 and 295 K.

T(K)	x	IS(mm/s)	QS(mm/s)	H_{hf} (T)	FWHM(mm/s)
295	0.0	0.36	0.0005	49.7	0.172
	0.10	0.37	-0.004	49.9	0.177
	0.15	0.37	-0.0002	49.7	0.167
	0.20	0.37	0.0018	49.7	0.161
78	0.0	0.47	0.0043	54.4	2.52
	0.10	0.47	0.009	54.6	2.7
	0.15	0.46	0.01	54.6	2.66
	0.20	0.46	0.0089	54.6	2.71

The isomer shift values in $Y_{1-x}Bi_xFeO_3$, within the experimental error, are practically the same as those related to trivalent iron in these structures. The quadrupole splitting values are about zero, and indicate that the Fe^{3+} ions are almost at the symmetrical position.

TEM images of the samples with different x values are illustrated in Figs. 4a to 4d, indicating the

nanoscale nature of orthoferrites particles. The images also show that mean particle sizes of the powders are about 75 nm. TEM image of the sample with $x=0.2$ with a higher magnification is shown in figure 4e, which shows that there are some fine spherical particles (about 4 nm in diameter) dispersed in large particles.

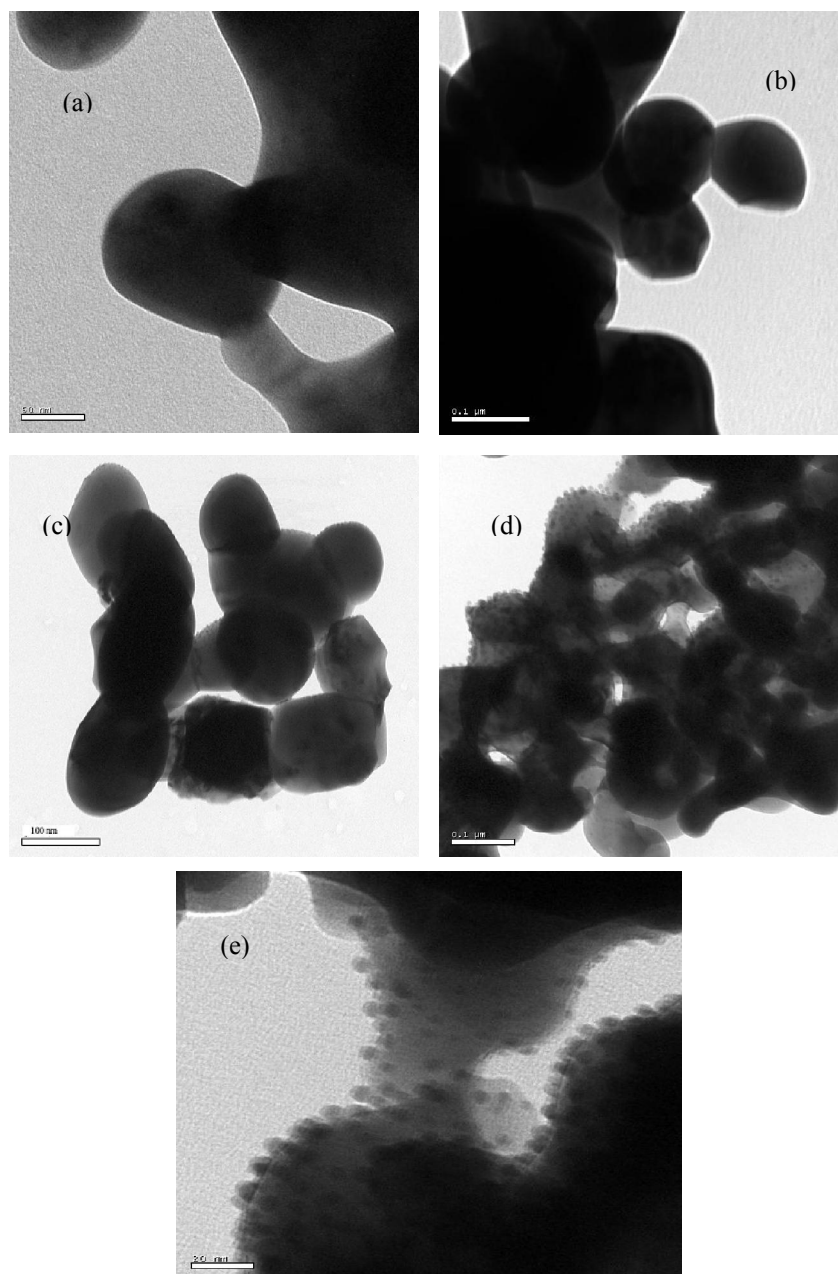


Fig.4. TEM images of the samples with (a) $x=0$, (b) $x=0.1$, (c) $x=0.15$, (d) and (e) $x=0.2$.

Room temperature hysteresis loops of the samples with $x=0$, 0.1 and 0.15 are shown in figure 5a, which shows that the magnetizations do not saturate up to maximum applied field of 13.5 kOe. The magnetizations of the samples with $x=0$, 0.1 and 0.15 at the maximum measuring field (13.5 kOe) are 0.58, 0.64 and 1.66 emu/g, respectively. This

indicates that the magnetization increases as Bi content increases. This increase is due to an increase in canting angle (Equation 1), resulted from disturbance of orthoferrite structure because of substitution of smaller yttrium ions by larger bismuth ones.

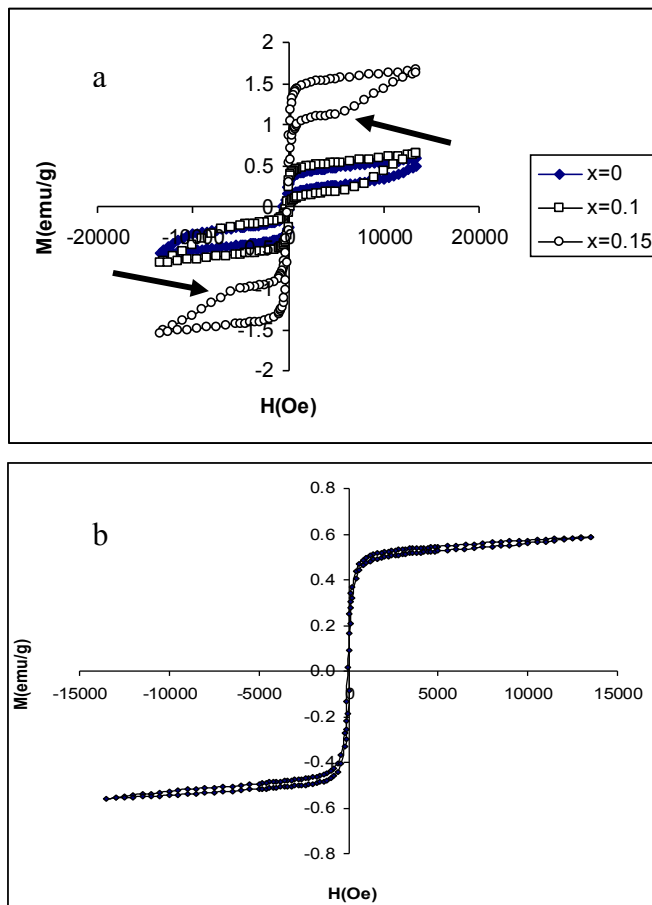


Fig.5. M-H curve of the samples with a) $x=0, 0.1$ and 0.15 , b) $x=0.2$.

Fig. 5b shows room temperature hysteresis loop of the sample with $x=0.2$. The magnetization of the sample at the maximum applied field (13.5 kOe) is 0.56 emu/g. This is even lower than the magnetization of the sample with $x=0$ obtained at the same applied field. This decrease is due to the presence of a great lot of fine spherical particles (Fig. 4e), which can be explained according to the core-shell model [11].

Hysteresis loops of the samples show a linear decrease starting from maximum magnetic field (13.5 kOe). This decrease can be explained by analogy to the case of a simple antiferromagnet, in which when the applied field is perpendicular to the easy axis, magnetization increases linearly [3]. As a powder is composed of randomly oriented crystallites, when it is exposed to a high applied field, magnetic moments of the crystallites will rotate, so that their directions become perpendicular to the field direction. This is due to the fact that this state has a lower energy than the state, in which the moments are oriented related to applied field randomly. So by decreasing the applied field the magnetization decreases linearly [12] to about zero. By reversing the magnetic field

and in low field region a sudden moment flopping will occur [13].

For the samples with $x=0, 0.1$ and 0.15 , the magnetization slopes with respect to field ($\frac{\partial M}{\partial H}$) which are obtained in the linear part of the curves are nearly equal to 1.3×10^{-5} emu/gOe. This feature can be correlated to a strong AF interaction dominated by the interaction of Fe^{3+} - Fe^{3+} pairs [14]. For the sample with $x=0.2$, the slope $\frac{\partial M}{\partial H}$ is equal to 0.6×10^{-5} emu/gOe, which is smaller than that related to the first three samples, indicating that here the AF coupling is weaker.

Also there is a change in the slopes of the hysteresis loops, as labeled by arrows on the one of the M-H curves in Fig. 5a. This is due to transition from antiferromagnetic to ferromagnetic orders, which is known as metamagnetism [15].

The temperature dependence of the magnetization curves of $\text{Y}_{1-x}\text{Bi}_x\text{FeO}_3$ in an applied field $H=13.5$ kOe is shown in Fig. 6a.

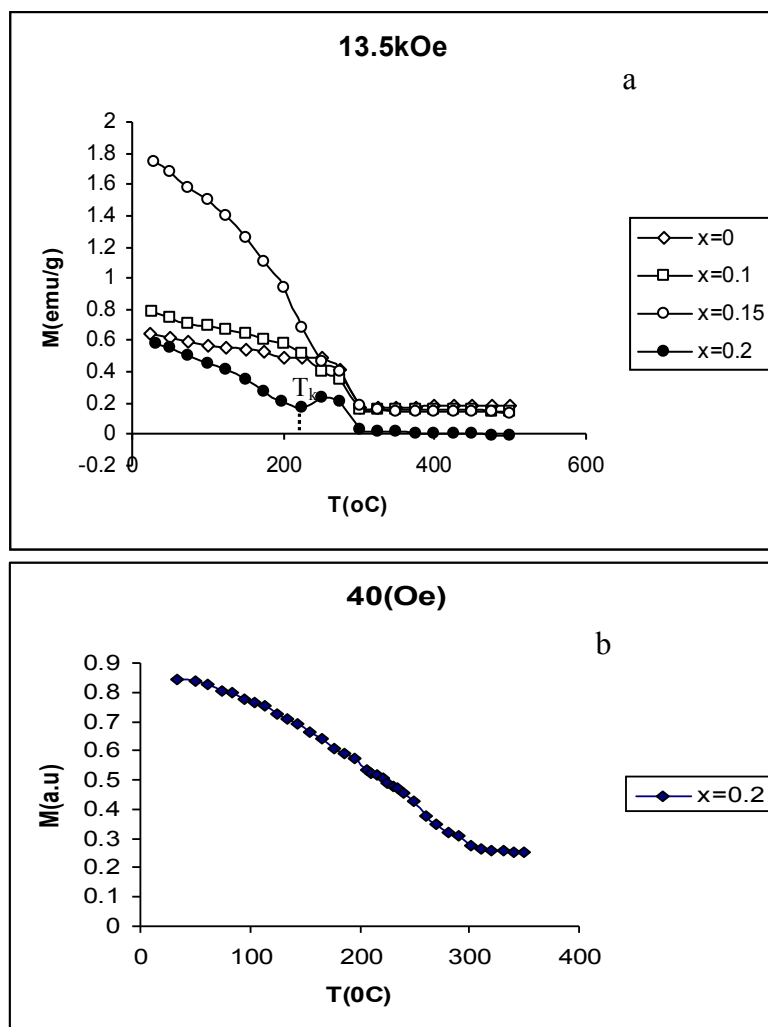


Fig.6. M-T curves of the all samples in an applied field of 13.5 kOe (a) and that of the sample with $x=0.2$ in an applied field of 40 Oe (b).

As can be seen by increasing of the temperature a transition from ferromagnetic to paramagnetic is observable for all the samples. The corresponding transition temperature (T_c) is constant as the Bi content increases. This is probably due to the fact that by substitution of bismuth in yttrium orthoferrites, the lattice structure disturbance increases and by which canting angle increases and the superexchange bond angle becomes smaller than 180° which will lead to an increase in superexchange energy [15]. On the other hand by substitution of Bi with larger ionic radius for Y with smaller ionic radius, the lattice volume increases and J_e (superexchange integral) reduces [12]. These two opposite effects could cancel out each other and the Curie temperature which is strongly depended on superexchange force remains constant. In the sample with $x=0$ the Curie temperature is about 573K that is 70K lower than the T_c of bulk sample. This decrease is probably due to

the decrease in particle size in which the ratio of surface atoms to the volume ones is increased and the number of superexchange interactions per unit volume is decreased, so Curie temperature should be decreased [16].

There are also peaks on all M-T curves ($H=13.5$ kOe) of the sample about $T=250^\circ\text{C}$, which is more remarkable for the sample with $x=0.2$. This maximum can be attributed to Hopkinson's peak, which is a character of ferromagnetic materials [17]. The peaks were not observed at low applied field (40 Oe), as shown for the sample with $x=0.2$ in Fig. 6b. This means that this field is not sufficient to make the magnetic moments parallel to the applied field to achieve a higher magnetization.

Conclusion

In this paper it was shown that single phase orthoferrite nanopowders can be prepared by the sol-

gel method. Magnetization increases as Bi content increases up to $x=0.15$ and a spin flopping or swinching behavior was observed around the origin of the hysteresis loops. Also a metamagnetic behavior was observed on the loops. The Curie temperature seems to be governed by the superexchange interaction and Hopkinson's peaks were detected for all the samples, which was more remarkable for the sample with $x=0.2$.

Corresponding author

Azar. Beiranvand

Department of Physics, Faculty of Science, Korram Abad branch, Islamic Azad University, Korram Abad, Lorestan, Iran

Email: a.beyranvand@gmail.com

References

1. M. Eibschutz, S. Shtrikman, D. Treves, Phys. Rev. **156**, 562 (1967).
2. S. Mathur, M. Veith, R. Rapalaviciute, H. Shen, J. Chem. Matter. **16**, 1906 (2004).
3. E. Lima, T. B. Martins, G. F. Goya, J. Magn. Mater. **320**, 622 (2008).
4. D. Treves, J. Appl. Phys. **36**, 1033 (1965).
5. M. Rajendran, A. K. Bhattacharya, J. Euro. Ceram. Soc., **26**, 3675 (2006).
6. F. J. Kahn, P. S. Pershan, J. P. Remeika, Phys. Rev. Lett. **186**, 891 (1969).
7. S.L. Samal, W. Green, S.E. Loflandc, K.V. Ramanujachary, D. Das, A.K. Ganguli, J. Solid State Chem. **181**, 61 (2008).
8. M. Rajendran, M. G. Krishna, A. K. Bhattacharya, J. Thin Solid Films, **385**, 230 (2001).
9. D. S. Todorovsky, R. V. Todorovska, S. G. Zotova, J. Mater. Lett. **55**, 41 (2002).
10. R. Mishra, K. Pradhan, R. Choudhary, A. Banerjee, J. Phys.: Condens. Matter **20**, 045218 (2008).
11. M. Muroi, R. Street, P. G. McCormick, J. Amighian, Phys. Rev. B, **63**, 184414 (2001).
12. A. H. Morrish, Wiley-IEEE Press (January 1, 2001).
13. B. D. Cullity, Addison Wesley Inc. (1972).
14. K. Bouziane, A. Yousif, J. Appl. Phys. **97**, 10A504 (2005).
15. S. Chikazumi, John Wiley & Sons Inc. (1964).
16. D. Zhang, K. J. Klabunde, C. M. Sorensen, G. C. Hadjipanayis, Phys. Rev. B, **12**, 14167 (1998).
17. H. Pfeiffer, W. Schüppel, J. Magn. Mater. **130**, 92 (1994).

3/5/2013